Right Place, Right Time! Dynamizing Topological Graphs for Embodied Navigation

Vishnu Sashank Dorbala[*] Bhrij Patel[*] Amrit Singh Bedi Dinesh Manocha

University of Maryland, College Park

Abstract

Embodied Navigation tasks often involve constructing topological graphs of a scene during exploration to facilitate high-level planning and decision-making for execution in continuous environments. Prior literature makes the assumption of static graphs with stationary targets, which does not hold in many real-world environments with moving objects. To address this, we present a novel formulation generalizing navigation to dynamic environments by introducing structured object transitions to dynamize static topological graphs called Object Transition Graphs (OTGs). OTGs simulate portable targets following structured routes inspired by human habits. We apply this technique to Matterport3D (MP3D), a popular simulator for evaluating embodied tasks. On these dynamized OTGs, we establish a navigation benchmark by evaluating Oracle-based, Reinforcement Learning, and Large Language Model (LLM)-based approaches on a multi-object finding task. Further, we quantify agent adaptability, and make key inferences such as agents employing learned decision-making strategies generalize better than those relying on privileged oracle knowledge. To the best of our knowledge, ours is the first work to introduce structured temporal dynamism on topological graphs for studying generalist embodied navigation policies. The code and dataset for our OTGs will be made publicly available to foster research on embodied navigation in dynamic scenes.

1. Introduction

Embodied navigation tasks often rely on topological graphs (TGs) for decision-making. Visual-Language Navigation (VLN) tasks such as REVERIE [36] and R2R [2, 11] utilize TGs extracted from MP3D [8] to follow human guidance. Similarly, methods for ObjectNav, PointNav, and ImageNav often employ TGs [10, 14, 20, 22, 38, 53, 55], where nodes represent locations or landmarks, and edges define traversable paths. These graphs provide a structured way to plan and execute navigation policies.

A key limitation of these existing embodied navigation paradigms is their reliance on static graphs, where objects within nodes remain stationary. This static assumption is unrealistic, as real-world environments are inherently dynamic, where users frequently move small, portable objects from place to place, such as shifting their phone or wallet between rooms throughout the day. Studies on robots in collaborative environments [3, 16, 34] suggest that human object placements follow structured patterns shaped by routines and habits, introducing a degree of entropy in object locations over time. Despite this, existing navigation benchmarks fail to model such temporal variability, limiting their applicability for real-world deployment.

In the ObjectNav task [4, 18] for instance, common state-of-the-art navigation approaches involve Reinforcement Learning (RL) [4, 47, 52, 54] and LLM-based zero-shot methods [6, 18, 45] to find stationary objects. RL policies for multi-object settings [9, 50] have also been introduced, but these are also based on static environments. For real-world deployment, these approaches must *generalize*, or maintain performance in dynamic scenes with shifting targets. Generalizability in prior embodied work has been described in terms of measuring an agent's capacity to adapt to novel settings, but this usually refers to *static* environments that were unseen or used synthesized guidance language [17, 23, 26, 57]. However, there has been little to no work that defines generalizability in the context of adapting to dynamic settings with moving objects. The evaluation of these prior approaches on dynamic settings with *non-stationary objects* remains to be seen.

To address this gap, in this work, we introduce Object-Transition Graphs (OTGs), a dynamic variant of topological graphs that incorporates *structured* object transitions over time. Figure 1 illustrates this concept. Unlike traditional TGs, where navigation is performed on a static graph, OTGs introduce a temporal component, where objects shift positions while the underlying graph structure remains constant. This forces an agent to synchronize its trajectory with tem-

[*]Equal contribution.

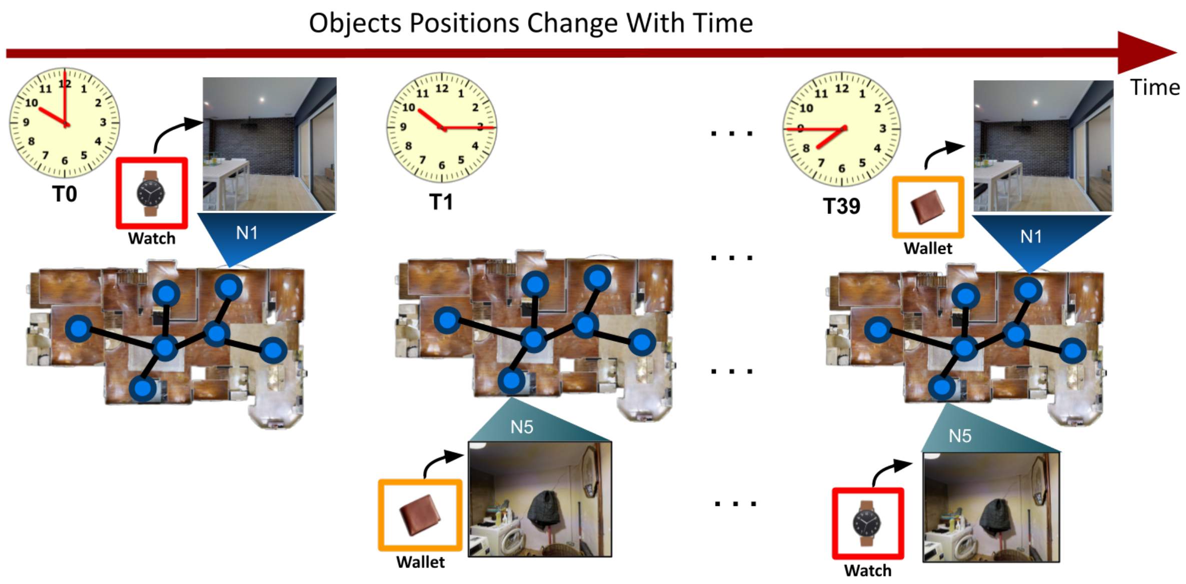

Figure 1. **Object Transition Graph (OTGs)**: We introduce dynamism to topological graphs via portable targets following structured object transition scenarios. In this representative figure, the watch (in red) moves from node *N1* at *T=10:00 AM* to node *N5* at *T=7:45 PM*, while the wallet (in orange) moves from node *N5* at *T=10:15 AM* to node *N1* at *T=7:45 PM*. We study the performance of various navigation agents in different object transition scenarios, and establish their generalizability.

poral object movements; its adaptability to change allows us to measure its generalist navigation performance. In dynamizing static topological graphs, our work seeks to redefine how we evaluate decision-making on embodied agents, by emphasizing not just **where** to navigate but also **when**.

In this work, we define the generalizability of a navigation approach by comparing the performance between static TGs and their OTG counterparts. This allows us to quantify an agent's robustness to dynamic changes, providing us with key insights on the effectiveness of graph-based navigation schemes in real-world settings.

Main Results. We generalize embodied navigation to dynamic environments by 1) introducing structured object transitions to make static topological graphs dynamic, and 2) presenting a benchmark for evaluating the adaptability of state-of-the-art navigation policies in such dynamic settings. Our contributions are summarized as follows:

- **Dynamizing Topological Graphs:** We propose a novel framework for introducing *structured* object transitions on static topological graphs, transforming them into Object Transition Graphs or OTGs. Inspired by human habits, our approach defines three distinct **object transition scenarios** to govern the movement of small, portable objects in a scene, providing varying levels of entropy. Our method applies to any static topological graph, including those obtained from Matterport3D (MP3D) [8] and HM3D [37]. Our dynamized MP3D environments and code will be released as an open-source benchmark to foster research in this area.
- **OTG Benchmark:** We introduce a benchmark for evaluating navigation performance on OTGs, comparing heuristic, RL, and LLM-based agents across structured object transition scenarios on a multi-object finding task. Measuring performance of agents on OTGs provides insights into the adaptability of graph-based approaches in dynamic environments with non-stationary objects.
- **Generalization in Dynamic Environments**: We make several key inferences on the generalizability of various navigation approaches by comparing their performance on OTGs against static TGs. In particular, we observe that strategies relying on privileged knowledge can lead to suboptimal decision-making in dynamic environments, while approaches that improve agents with experience and collected observations better generalize to OTGs.

2. Related Works

Traditionally, navigation in dynamic environments has focused on *low-level* planning tasks, such as crowd avoidance [5, 31, 41] and socially aware navigation [7, 29], where agents continuously maneuver to avoid obstacles while minimizing trajectory length or time. In contrast, embodied navigation tasks employing *high-level* planning on graphs are predominantly studied in static environments, with limited research on handling dynamic targets [11, 44]. With OTGs, we introduce a form of structured temporality in dynamic environments where agents must reason over spatio-temporal changes, extending high-level planning to dynamic scenes with shifting targets. While recent simulators like Habitat 3.0 [35] include object rearrangement tasks, these primarily focus on agents modifying the envi-

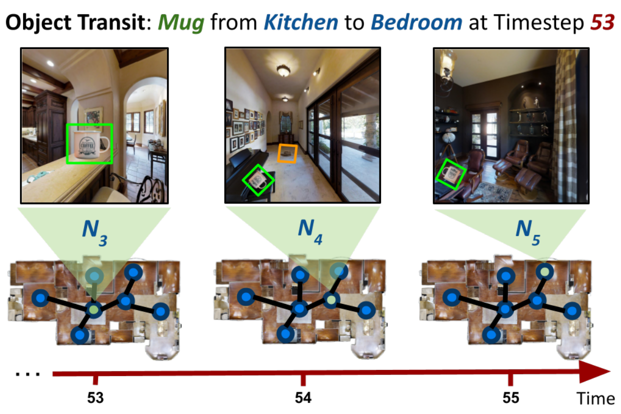

Figure 2. **Object Transition**: Portable objects move around the scene at various timesteps in accordance to their natural rooms (Table 1) and transit scenarios (Table 2). Here, a *mug* is placed on a kitchen node N_3 at timestep $T = 53$, but moves to a bedroom node N_5 at timestep $T = 55$ via node N_4. If an agent reaches the kitchen after $T = 53$ (or the bedroom before $T = 55$), it would fail to see the mug. Multiple objects could also be at the same node (hat and mug in $N4$).

ronment rather than adapting to dynamic object placements over time.

Planning in dynamic environments has been studied in the past [32, 48, 59], with recent approaches even utilizing LLMs in conjunction with multi-arm bandits [15]. These schemes usually propose memory augmentations with hierarchical planning procedures and frame the problem from an obstacle avoidance standpoint [25, 48, 58]. In contrast, our work considers the case where the objects themselves are non-stationary.

Rudra et al. [40] define small portable objects around the house and propose a contextual bandit scheme that aims to learn the likelihood of finding an object at various waypoints. In their case, however, object locations are shuffled only after each episode, meaning it finally boils down to an object-finding navigation task in a static environment. In contrast, we tackle a *truly* dynamic case, where objects are moving even *during* the episode. This definition adds a layer of complexity as the embodied agent must now navigate towards a constantly shifting target object, for which it needs to identify specific routines and object movement patterns in the environment.

Kurenkov et al. [21] introduced dynamizing household environments and experimented with scene graph memory to predict object locations. They also performed target object-finding experiments, but the environment was static as the agent moved. In our work, the objects move as the agent moves, and we deal with topological graphs, not scene graphs. Furthermore, Wang et al. [49] used LLM-generated human activities to dynamize a topological graph of a household environment and performed ObjectNav experiments in these environments. In contrast, our work focuses on converting topological graphs into object transition graphs, and comments on the generalizability of embodied navigation approaches in dynamic environments.

3. Object Transition Graph (OTG):

We define Object Transition Graphs (OTGs) is an evolutionary undirected graph where the underlying graph structure remains constant, but the objects present in its nodes evolve over time. Formally, let $G = (V, E)$ be a topological graph structure with nodes V representing spatial locations (rooms and objects), and edges E representing traversable paths between the nodes. Let $\mathcal{O}$ represent the total set of available portable objects. Then, at each timestep t, $v \in V$ is associated with a set of portable target objects $O_v(t) \subseteq \mathcal{O}$. While the graph topology remains static, the object assignments $O_v(t)$ evolve via a time-dependent transitioning style Λ, to give us an object transition function O as,

$$O : V \times \Lambda \rightarrow 2^{\mathcal{O}} \tag{1}$$

where $2^{\mathcal{O}}$ is a power set representing all possible portable object combinations. At each timestep t, $O(v,t)$ gives us the portable targets present in each node v based on the transition style Λ.

3.1. Defining Transition Scenarios Λ:

Human habit formation via object placement can be attributed to *cognitive offloading*, where individuals rely on the environment to reduce memory demands [39, 46]. This reliance on the environment influences the spatial distribution of objects. Frequently used objects (like keys or phones) might move more flexibly across rooms (high entropy), while function-specific objects (like dumbbells or toothbrush) might be more constrained (low entropy). We use this structured transition behavior to define an object's *transition entropy*, which we use to formulate Λ. We consider three object transit scenarios at decreasing levels of *transit entropy*:- 1) **Random**, **Semi-Routine**, and **Fully-Routine**. These are outlined in Table 2.

Algorithm 1 describes our approach for generating an evolving graph trajectory ζ to dynamize any topological graph G. Figure 2 further illustrates this setup. The initial graph contains portable objects placed according to Table 1. We then generate ζ by moving objects in the graph at various timesteps for each transit scenario Λ. ζ is precomputed for each transit scenario and stored for later analysis with navigation algorithms.

When generating the evolving graph, a pseudo-random seed s helps differentiate the movement of portable objects

Room	**Portable Objects**
Bedroom	Charger, Water Bottle, Smartwatch, Laptop, Notebook, Toothbrush, Mug, USB Flash Drive, Phone, Headphones, Hat
Garage	Screwdriver, Flashlight, Mug, Phone, Headphones, Hat
Dining	Salt and Pepper Shakers, Portable Speaker, Charger, Water Bottle, Mug, Bowl, Phone, Headphones, Hat
Office	Charger, Laptop, Hat, Notebook, USB Flash Drive, Mug, Phone, Headphones
Bathroom	Toothbrush, Phone, First-Aid Kit
Kitchen	Salt and Pepper Shakers, Hat, Mug, Bowl, Phone, Headphones, First-Aid Kit
Lounge	Playing Cards, Mug, Portable Speaker, Charger, Water Bottle, Laptop, Phone, USB Flash Drive, Dice, Headphones, Hat
Gym	Dumbbells, Jumprope, Smartwatch, Phone, Headphones, Hat
Outdoor	Jumprope, Smartwatch, Portable Speaker, Phone, Water Bottle, Headphones, Hat
Recreation	Playing Cards, Dice, Water Bottle, Headphones, Hat

Table 1. **Rooms and Portable Objects**: We map 21 portable objects to a set of household rooms. This mapping is used to set destinations for object transit. During each episode, objects are placed in various rooms for a range of timesteps. Commonly moved objects such as *phone, headphones* are associated with 9 different rooms, while less commonly shifted ones such as *dumbbells* appear only in the Gym.

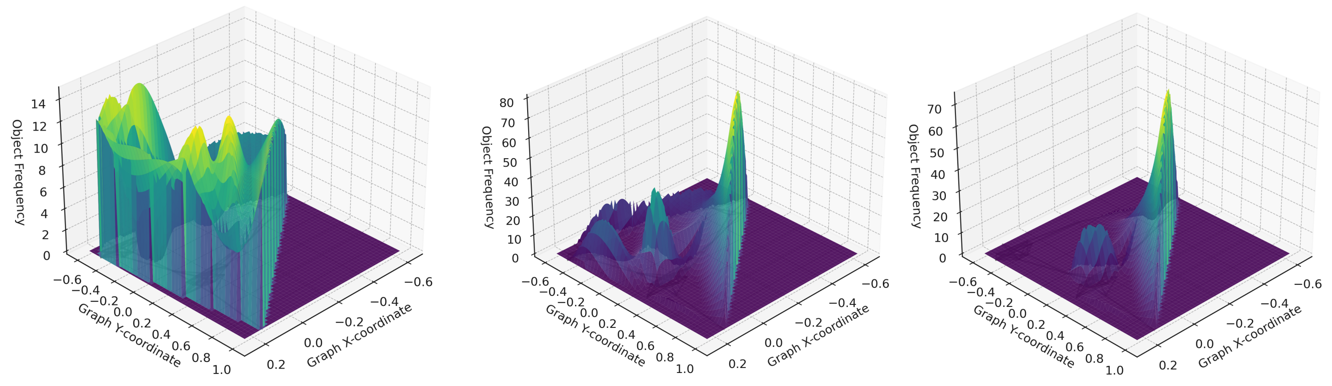

(a) Random Scenario (b) Semi-Routine Scenario (c) Fully-Routine Scenario

Figure 3. **Object Frequency Visualization**: A visual representation of portable target frequencies over several timesteps in various transit scenarios Λ. We simulate portable objects transiting on a topological graph from MP3D. In the random case, object frequencies are more scattered (high entropy); in semi-routine, target rooms are fixed, but paths are flexible (medium entropy); and in the routine case, both rooms and paths are fixed (lowest entropy). Note the distribution of object frequencies visually correlates to their entropy.

Scenario (Λ)	**Fixed Rooms**	**Fixed Paths**	**Entropy**
Static	✓	N/A	None
Random	✗	✗	High
Semi-Routine	✓	✗	Medium
Fully-Routine	✓	✓	Low

Table 2. **Object Transit Scenarios Λ**: Portable targets transition in the graph under structured scenarios inspired by human habits. In the random case, the portable objects can move to any room at any time during each episode. In the routine cases, the rooms that the target objects can travel to are fixed (except during transit). The static scenario is a baseline with stationary items i.e., zero entropy.

per episode. Letting e be the episode index,

$$s = \begin{cases} 1 \text{ (or fixed)} & \text{if movement is fully routine,} \\ e & \text{if movement is random or semi-routine.} \end{cases} \tag{2}$$

Note that for the fully routine case, ζ remains constant for all episodes of the experiment, meaning that the object transition routes remain fixed. In the other two cases, ζ varies per episode according to the room and interval variability described. Figure 3 presents a visual representation of the object frequencies in all three scenarios.

For our experiments, we dynamize topological graphs obtained from the Matterport3D (MP3D) [8] dataset using Algorithm 1 to obtain OTGs. Each node contains panoramic images representing the scene, and edges represent the distance between them. Additionally, we have the room type for each node and use them as a template to define the set of portable objects listed in Table 1.

Note on Visual Spatial Placement. Beyond object transitions, we also investigate spatial transformations in placing the objects on the scene. Portable objects are small and can be pasted on the scene in various ways. We first use Fast-

SAM [56] to obtain segmentation masks for both the scene and the portable target object. On the scene segmentations, we filter out a set of K largest segments below the center of the image, to avoid placing floating targets. We then place the target objects on a randomly chosen segment $k \in K$ this set. This simple placement technique for small objects allows us to modify images of pre-existing topological graphs and makes the visual grounding task challenging enough for comparison against various backgrounds. While 3D object placement would be more accurate, this is more cumbersome to setup, and is tangential to the focus of this paper, which is to introduce OTGs to study navigation generalizability. More details on our visual grounding experiments with VLMs can be found in the Appendix. We will be releasing this dataset of small objects placed on MP3D to foster research in embodied visual grounding.

4. Task: Multi-Object Finding

To evaluate how well different navigation methods perform on dynamic OTGs, we aim to assess their generalizability. Given a topological graph, the generalizability is the difference in performance achieved by a navigation scheme between when then graph is static and when the graph is dynamic. For example in Section 6, we measure the generalizability of PPO-based agents by training an agent in a static environment and training another in a dynamic environment and compare the difference in performance.

Algorithm 1 Modify G With Object Transitions Λ

Input: Topological Graph $G = (V, E)$, Portable Object Set $\mathcal{O}$, Episode Length T, Initial Agent Node r, Object Density d, Object Transit Scenario Λ, Local Graph Size q.
Output: Evolving Graph Trajectory ζ
Initialize: Add $\mathcal{O}$ portable objects to G_0. Calculate the object density d of the local graph g around the initial node r. g is all nodes within q steps of r.
Sample $N \in \mathcal{O}$ duplicate new objects and add them to random nodes in g to match required density d. $\mathcal{O}' = \mathcal{O} + N$ is the total set of objects at G_0

```
1:  for $t \in [1, \ldots, T]$ do
2:      $G_t = G_{t-1}$
3:      for each object $o \in \mathcal{O}'$ do
4:          Using Equation 1: $O(v, t) \leftarrow O(v, \Lambda)$
5:          Sample $v_k \in V$ from $O(v, t)$ {Following $\Lambda$}
6:          if $v_k \neq v_o$ then
7:              if $\Lambda =$ Fully-Routine then
8:                  Use fixed trajectory $\delta(t)$
9:              else
10:                 Compute random path $\delta(t)$ from $v_o$ to $v_k$
11:             end if
12:             Move $o$ along $\delta$ to $v_k$ over $t$ timesteps
13:         end if
14:     end for
15:     Add $G_t$ to $\zeta$
16: end for
17: return $\zeta$
```

To enable this study, we focus on the task of finding multiple portable target objects over a fixed timespan. This setting adds realism to other multi-object finding tasks such as Multi-ON [50] and GOAT [9] by introducing non-stationary targets. For dynamic settings such as ours, we argue that a multi-object finding task is preferable over a standard single-object finding setup for two reasons:-

- **Realistic Setting**: In real-world homes, users frequently move objects, leading to dynamically changing object locations [3, 34]. Assistive agents must track and infer object movements over time to provide meaningful assistance. This requires monitoring *multiple* portable objects (e.g., phones, watches) rather than treating each search as an isolated event.
- **Lifelong Navigation**: A multi-object setup enables an agent to finetune its search policy in real-time, by using knowledge gathered from finding previous objects to better find the next. An agent deployed at homes will likely have to face similar conditions, with a user asking it to find multiple targets without 'resetting' its position, much akin to lifelong navigation [53].

First, we mathematically formalize what navigating on an OTG entails. Let Λ describe the transitory motions of objects. Then, let O be the set of portable objects found over T timesteps for an agent starting at node r with an object distribution density d. Then $S = [r, d, T, \Lambda]$ represents a set of our experimental variables for this task. We then define our navigation objective as *"Finding the **maximum** number of portable objects O while traversing a dynamic environment represented by S."*.

For downstream applications like embodied agents personalizing to households, we believe finding multiple targets to be a good task to study dynamic adaptability, due to dense reward signals [9]. The setting is also realistic as households have multiple people moving objects around at the same time. We study the performance of different navigation policies with varying simulator conditions S.

In each episode, the agent is tasked with finding as many portable target objects as possible by making decisions on a dynamic OTG. Let τ be a finite trajectory representing a sequential list of visited nodes on the OTG, G, and let $\tau(t)$ be the t-th node in τ. We can now define $O(\tau, t)$ as the set of portable objects found at the t-th node of τ at time t. Given that the objects move throughout the scene, the t-th node may have a different set of portable objects present at a different timestep. Given a trajectory τ of length T, we can formulate the total set of portable objects found along τ as $O_\tau = \cup_{t=1}^{T} O(\tau, t)$.

A navigation agent parameterized by policy π explores the dynamic OTG by generating a trajectory τ_π, where each timestep t corresponds to a selected node: $\tau_\pi(t) \in V$. Specifically, $\tau_\pi(t)$ is the node chosen at time t by policy π. We now can write the policy optimization problem as finding an optimal policy π^* defined as $\pi^* = \arg\max_\pi |O_{\tau_\pi}|$.

Consequently, $O_{\tau_{\pi^*}}$ is the maximum number of portable targets that can be found by taking the optimal trajectory. In the following section, we describe various navigation schemes that we employ to perform the multi-object finding task on OTGs.

5. Navigation Approaches

To infer the generalizability of prior navigation models, we emulate a static topological graph environment by keeping portable objects stationary in one location throughout the experiment. We then evaluate both the static topological graph environment and the dynamic OTG environment with 5 relevant navigation agents.

Random Agent. For a completely random navigation baseline, at each timestep t, the agent chooses one of its neighboring nodes to go to for the next iteration.

Oracle Agent. We utilize a greedy heuristic on an agent as an oracle baseline: At each timestep $t \in [1, T]$, we perform a Breadth-First Search (BFS) to find the closest node with an unseen portable object. Using the shortest path between the unseen object and its current position, the agent then moves its neighboring node on the given shortest path. This approach relies on the agent having access to an "oracle" that tells it about the closest node containing a unique portable target at a given timestep. While oracle knowledge is useful since the position of the objects in the environment changes with time, note that there is a possibility that it will not find an object after navigating to an oracle-guided node.

Reinforcement Learning Agent. We use a reinforcement learning-based method, specifically Proximal Policy Optimization (PPO) [43] to define an agent. PPO has been used in several previous works in embodied navigation tasks, such as ObjectNav [51, 54, 60] with SOTA results.

Observation Space: Given the limited prior literature dealing with PPO on a dynamic topological graph, we consider constructing our agent with the following observation space as input to the navigation agent. To define the observation space, let $|G|$ be the number of nodes on G, and each node is given a unique ID from $\{0, \dots, |G| - 1\}$:

- Current timestep, $t \in T$
- ID the current node, n_t from a list of all nodes in the environment graph
- A list with each index corresponding to a node ID. The element at a given index is the number of objects at the corresponding node at timestep t

Action Space: The PPO agent then outputs the index of the node it wants to travel to for the next timestep $t+1$. We use a Maskable PPO to only allow it to choose neighboring nodes. The mask in this case is a list with each index corresponding to a node ID. The element at a given index is either 1 if it is a neighbor of the current node and 0 otherwise.

Reward Objective: Let O_{t-1} be the set of distinct portable objects the agent as seen up to time $t-1$. The reward is the number of new objects it has found at the current node n_t that are not in O_{t-1}. Formally, the reward at timestep t is $|O(n_t) \setminus O_{t-1}|$.

Note. Our version of PPO uses a map of the environment and the number of objects at each node at each timestep.

LLM-based Agents. For LLM-based navigation, we consider two variations of LGX [18], an LLM-based method for zero-shot embodied exploration.

1. LLM-Vanilla: Given a target object, the LLM takes a list of objects around the agent and asks an LLM (GPT-4o) to predict an object to navigate toward. The agent then navigates towards the predicted object and continues doing so till the provided target is found.

The LLM's prompt contains a set of portable targets remaining to be found in the environment. At each timestep, we use YOLO v8 [19] to obtain a list of objects in the scene, and then prompt GPT-4o with the object list asking for an object prediction from the list that might lead to an unseen portable object. We then use the MP3D topological graph to hop to the next node.

2. LLM with Memory: The vanilla version of the LLM agent works in a zero-shot manner resembling a Markov Chain, meaning that it makes navigation decisions at each node solely based on the observations it has seen at the current timestep. Since objects keep transiting on our OTG, keeping track of previously seen objects should help the agent make more prudent navigational decisions.

We accommodate this by incorporating memory by passing a set of historical objects seen, predictions made, and timesteps to the prompt across episodes. The system prompt contains this historical data, along with a set of portable objects remaining to be found in the environment. We maintain a horizon to avoid GPT token overflow, where we remove the earliest appended observation when an overflow of tokens occurs.

6. Experiments and Results

We treat navigating in dynamic scenes and visual target grounding as separate problems in our experiments. This decoupling allows us to individually analyze navigation and grounding performance. The results of our visual grounding experiments are explained in detail in the supplementary.

6.1. Hyperparameters

We determine 4 hyperparameters that influence performance as described in the definition section, i.e., $S = [r, d, T, \Lambda]$. Each agent is subjected to a total of $[Stationary(1) + Transit(3)] \times R \times E \times T$ experiments, where R is a set of rooms that varies with each scan from which a random node $r \in R$ is picked as a starting point for each trial. The maximum number of trials is thus equal to the number of rooms. R ranges from $[11, 30]$ in our chosen subset of 10 MP3D scans. E is the number of episodes that we run for each starting node r, and T is the number of timesteps per episode. We set $R = 10$, $E = 20$ and $T = 30$ in our experiments. Although different objects can have different levels of transition entropy, we set all objects in an experimental run to have the same transit scenario Λ. Setting all objects to have the same transit allows us to better analyze the generalizability of a navigation scheme in different levels of entropy in the OTG.

Ground Truth Paths (Π^*). Given a starting node $r \in R$, for each episode $e \in E$, there exists a set of ground truth paths Π^* over T that the agent could take for collecting the most number of portable targets. We compute these paths by simulating all possible trajectories from a given starting point r, and store Π^* to calculate performance and efficiency later.

Object Density d. To make the MP3D environment less sparse with objects, we define a local graph of all nodes within 3 steps away from the agent's initial node. We then populate the local graph by adding duplicate portable objects from O to the local graph. We populate until the object density d of this local graph is 1. As in, on average, each node in the local graph has 1 object. In Algorithm 1, d and the local graph size q are hyperparameters.

6.2. Evaluation Metrics

Success Rate (SR): Given an episode, we measure the object-finding performance of an agent by dividing the number of objects found in that episode by the maximum possible number of objects that could have been found with a ground-truth path $\pi^* \in \Pi^*$: $SR = |O_\pi|/|O_{\pi^*}|$. This metric is similar to the Progress metric in Wani et al. [50]. In this work, the ground-truth trajectory may not necessarily find all the objects in the given timeframe.

Trajectory Alignment (TA): To measure path efficiency, we define Trajectory Alignment as the average overlap between ground-truth trajectory π^* and trajectory taken by the agent across episodes. We take the maximum across Π^*: $TA = \min_{\pi^* \in \Pi^*} \frac{1}{T} \sum_{t \in T} \mathbf{1}_{\pi(t)=\pi^*(t)}$, where $\mathbf{1}$ is an indicator function.

Relative Change in Success (RCS): We use this value taken from [17] to measure the generalizability from static to dynamic environments. It is the percent relative change between static and dynamic navigation performance. We measure RCS for various Λ cases and report scores on SR and SPL. Lower values indicate better generalizability, showing that the agent performance between static and dynamic environments is consistent.

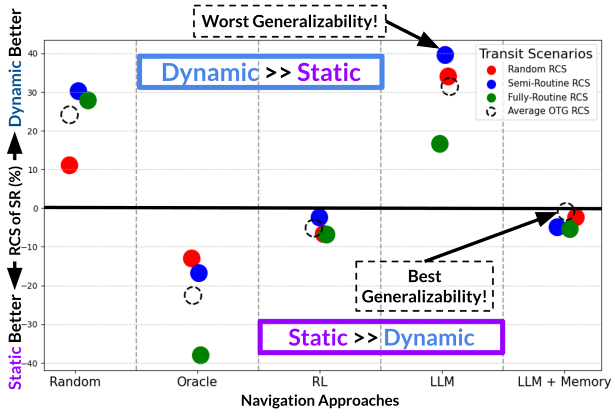

Figure 4. Navigation Generalizability on OTGs (RCS): Relative Change in Success (RCS) measures an agent's adaptability, comparing dynamic to static TG performance (optimal RCS is 0%). Positive values indicate better dynamic performance (chance encounters), while negative values reflect poor adaptability. Experiential-learning methods (RL, LLM+Memory) approach optimal RCS, demonstrating better generalization, while the Oracle and Vanilla LLM perform poorly.

6.3. Navigation Inference

Table 3 presents the results of our agents on the navigation task on OTGs. We run experiments on 10 Matterport3D scans, with 10 randomly selected starting nodes $r \in R$, 20 episodes, and each episode having 20 timesteps. There are 4 key inferences from these observations to understand the generalizability of the various navigation approaches:

Experiential Navigation Approaches Generalize Well: Figure 4 presents a comparison of all approaches on RCS. LLM + Memory and PPO both have a relatively low RCS score, meaning that navigation agents perform comparably in stationary graphs and OTGs. Both methods rely on past observations to improve their decision-making, showing that data-driven approaches can be generalizable well. In contrast, the greedy heuristic Oracle agent and the zero-shot Vanilla LLM lack experience or memory, with the former relying on privileged knowledge and latter utilizing learned commonsense cues for decision-making. This result highlights *learned* decision-making improves generalizability, and we can infer this to be a key component for the real-world deployment of embodied agents.

Zero-shot Methods Camp to Find Objects: In the Vanilla LLM approach which is zero-shot without memory, we observe that the agent finds more objects in the OTG than in the static environment, as clearly indicated by the higher OTG SR scores across all Λs. In Table 3, we see that in the Fully-Routine case for Vanilla-LLM, the RCS for SR is $+16.7\%$ but the RCS for TA is -10.8%. These results suggest that while Vanilla-LLM is finding more objects in OTGs than in static environments, its trajectories show lesser overlap with the ground-truth paths (Π^*). Upon inspection, we observe that this agent has learned to *camp* at

Policy	**Metric (%)**	**Random Λ** Static	OTG	RCS (%)	**Semi-Routine Λ** Static	OTG	RCS (%)	**Fully-Routine Λ** Static	OTG	RCS (%)	**Avg. OTG** Static	OTG	RCS (%)
Random Agent	SR	66.0	74.4	+11.2	66.0	94.7	+30.3	66.0	91.6	+27.9	66.0	86.9	+24.1
	TA	33.5	24.4	−37.3	33.5	36.6	+8.4	33.5	33.6	**+0.29**	33.5	31.2	−6.8
Oracle Agent	SR	90.2	78.4	−13.0	90.2	75.1	−16.8	90.2	55.9	−38.0	90.2	69.8	−22.6
	TA	45.6	54.4	+16.2	45.6	50.6	+9.8	45.6	32.7	−28.3	45.6	45.9	**+0.6**
RL Agent	SR	59.1	55.2	−6.6	59.1	57.8	**-2.3**	59.1	55.2	−6.7	59.1	56.0	−5.2
	TA	41.6	37.3	−10.3	41.6	35.8	−14.0	41.6	32.1	−22.9	41.6	35.1	−15.7
Vanilla LLM Agent	SR	28.5	43.3	+34.1	28.5	47.2	+39.6	28.5	34.2	+16.7	28.5	41.6	+31.4
	TA	24.3	30.7	+20.9	24.3	31.3	+22.3	24.3	21.7	−10.8	24.3	27.9	+12.9
LLM + Mem. Agent	SR	50.6	49.4	**-2.4**	50.6	53.2	+4.8	50.6	47.9	**-5.4**	50.6	50.2	**-0.9**
	TA	36.9	33.8	**-8.5**	36.9	34.6	**-6.3**	36.9	32.4	−12.2	36.9	33.6	−9.0

Table 3. Navigation on OTGs: We evaluate 5 popular embodied navigation approaches on various OTGs, and also on a static graph. These values are used to compute RCS using the equation provided in [17]. An RCS value closer to 0% indicates good generalizability to new conditions. Highlighted in green are the best RCS values for SR, while ones in violet are the best values for TA. Observe that the LLM + Memory agent shows the best SR generalizability overall, followed very closely by the RL agent. Both these agents employ experiential learning to learn about object transit patterns and improve their performance.

privileged nodes that are in the paths of many object routes. One possible explanation is that the LLM is relying solely on common-sense knowledge and to go to areas where most objects can be found, rather than trying to learning object routes. We can consider camping as an instance of reward hacking, where we would not want an agent to camp at one location in anticipation of encountering a target. This challenge opens up exciting research directions in reward design for navigation on OTGs.

Greedy Heuristic Struggles With Shifting Objects: The navigation approach of the agent heavily relies on the static placement of objects to achieve high performance. This case is best shown in the Oracle agent. At each timestep, the oracle takes a step towards the closest target. However since targets are on the move, a greedy oracle tends to take a suboptimal path. The agent is heading in one particular direction towards a certain target object which was nearest, but then suddenly switches to another direction due to the nearest unseen object changing.

Entropy Influences Performance: In all policies barring the Random agent baseline, we observe that the performance on a Fully Routine Λ exhibiting low entropy is usually worse than the Semi-Routine or Random Λ cases. This is intuitive, and can be attributed to the agent encountering more targets in environments with higher object transit entropy. Despite this, we observe a strong performance of the RL agent in being entropy-agnostic, with very similar values across all transit cases on SR and SPL.

7. Conclusion, Limitations, and Further Work

We present Object Transition Graphs or OTGs, a generalization of the topological graphs to dynamic environments with shifting objects. Unlike static topological graphs where an agent is expected to navigate to *stationary* target objects, OTGs are realistic and challenging, with multiple portable objects transiting on a topological graph. Our dynamic task fundamentally challenges the static-scene assumption common in embodied navigation literature.

We first introduce a novel approach to transform topological graphs to OTGs by developing *structured* object transition scenarios inspired by human habits. Our approach can be used to transform any topological graph into an OTG, and we transform graphs extracted from MP3D for this purpose. On these OTGs, we measure the generalizability of various navigation approaches performing a multi-object finding task. In comparing performance on static TGs and OTGs, we infer the generalizability of these approaches to dynamic settings with non-stationary targets. We find that the type of navigation employed greatly influences agent performance, with experiential approaches that have the means to learn from memory generalizing the best. In one case, we notice an instance of reward hacking via *camping* behavior, motivating future research in reward design for OTGs. Code and data, including the dynamized MP3D dataset, will be made publicly available to foster research in this exciting new direction.

A limitation of our current setup is that we independently treat visually grounding small target objects as a separate problem. Coupling navigation on OTGs with visual grounding is a future direction. Another interesting direction in this regard is to utilize generative image modeling with OTG navigation on 2D simulators such as Minigrid [13], allowing us to scale up experimentation and training. Finally, our research paves the way for generalizability experiments in the context of dynamic scenes, and future work will look at studying the sim2real transfer of navigation policies trained on OTGs to a real world environment.

References

[1] Josh Achiam, Steven Adler, Sandhini Agarwal, Lama Ahmad, Ilge Akkaya, Florencia Leoni Aleman, Diogo Almeida, Janko Altenschmidt, Sam Altman, Shyamal Anadkat, et al. Gpt-4 technical report. *arXiv preprint arXiv:2303.08774*, 2023. 2

[2] Peter Anderson, Qi Wu, Damien Teney, Jake Bruce, Mark Johnson, Niko Sünderhauf, Ian Reid, Stephen Gould, and Anton Van Den Hengel. Vision-and-language navigation: Interpreting visually-grounded navigation instructions in real environments. In *Proceedings of the IEEE conference on computer vision and pattern recognition*, pages 3674–3683, 2018. 1

[3] Ermanno Bartoli, Fethiye Irmak Dogan, and Iolanda Leite. Streaming network for continual learning of object relocations under household context drifts. *arXiv preprint arXiv:2411.05549*, 2024. 1, 5

[4] Dhruv Batra, Aaron Gokaslan, Aniruddha Kembhavi, Oleksandr Maksymets, Roozbeh Mottaghi, Manolis Savva, Alexander Toshev, and Erik Wijmans. Objectnav revisited: On evaluation of embodied agents navigating to objects. *arXiv preprint arXiv:2006.13171*, 2020. 1

[5] Kuanqi Cai, Chaoqun Wang, Jiyu Cheng, Clarence W De Silva, and Max Q-H Meng. Mobile robot path planning in dynamic environments: A survey. *arXiv preprint arXiv:2006.14195*, 2020. 2

[6] Tommaso Campari, Leonardo Lamanna, Paolo Traverso, Luciano Serafini, and Lamberto Ballan. Online learning of reusable abstract models for object goal navigation. In *Proceedings of the IEEE/CVF Conference on Computer Vision and Pattern Recognition*, pages 14870–14879, 2022. 1

[7] Enrico Cancelli, Tommaso Campari, Luciano Serafini, Angel X Chang, and Lamberto Ballan. Exploiting proximity-aware tasks for embodied social navigation. In *Proceedings of the IEEE/CVF International Conference on Computer Vision*, pages 10957–10967, 2023. 2

[8] Angel Chang, Angela Dai, Thomas Funkhouser, Maciej Halber, Matthias Niessner, Manolis Savva, Shuran Song, Andy Zeng, and Yinda Zhang. Matterport3d: Learning from rgb-d data in indoor environments. *arXiv preprint arXiv:1709.06158*, 2017. 1, 2, 4

[9] et al. Chang, Matthew. Goat: Go to any thing. In *Robotics: Science and Systems*, 2024. 1, 5

[10] Devendra Singh Chaplot, Ruslan Salakhutdinov, Abhinav Gupta, and Saurabh Gupta. Neural topological slam for visual navigation. In *Proceedings of the IEEE/CVF conference on computer vision and pattern recognition*, pages 12875–12884, 2020. 1

[11] Kevin Chen, Junshen K Chen, Jo Chuang, Marynel Vázquez, and Silvio Savarese. Topological planning with transformers for vision-and-language navigation. In *Proceedings of the IEEE/CVF Conference on Computer Vision and Pattern Recognition*, pages 11276–11286, 2021. 1, 2

[12] Tianheng Cheng, Lin Song, Yixiao Ge, Wenyu Liu, Xinggang Wang, and Ying Shan. Yolo-world: Real-time open-vocabulary object detection, 2024. 2, 4

[13] Maxime Chevalier-Boisvert, Bolun Dai, Mark Towers, Rodrigo de Lazcano, Lucas Willems, Salem Lahlou, Suman Pal, Pablo Samuel Castro, and Jordan Terry. Minigrid & miniworld: Modular & customizable reinforcement learning environments for goal-oriented tasks. *CoRR*, abs/2306.13831, 2023. 8

[14] Xinru Cui, Qiming Liu, Zhe Liu, and Hesheng Wang. Frontier-enhanced topological memory with improved exploration awareness for embodied visual navigation. In *European Conference on Computer Vision*, pages 296–313. Springer, 2024. 1

[15] J de Curtò, I de Zarzà, Gemma Roig, Juan Carlos Cano, Pietro Manzoni, and Carlos T Calafate. Llm-informed multi-armed bandit strategies for non-stationary environments. *Electronics*, 12(13):2814, 2023. 3

[16] Douglas do Couto Teixeira, Jussara M Almeida, and Aline Carneiro Viana. On estimating the predictability of human mobility: the role of routine. *EPJ Data Science*, 10 (1):49, 2021. 1

[17] Vishnu Sashank Dorbala, Gunnar A Sigurdsson, Jesse Thomason, Robinson Piramuthu, and Gaurav S Sukhatme. Clip-nav: Using clip for zero-shot vision-and-language navigation. In *Workshop on Language and Robotics at CoRL 2022*, 2022. 1, 7, 8

[18] Vishnu Sashank Dorbala, James F Mullen Jr, and Dinesh Manocha. Can an embodied agent find your "cat-shaped mug"? llm-based zero-shot object navigation. *IEEE Robotics and Automation Letters*, 2023. 1, 6

[19] Glenn Jocher, Ayush Chaurasia, and Jing Qiu. Ultralytics YOLO, 2023. 6

[20] Nuri Kim, Obin Kwon, Hwiyeon Yoo, Yunho Choi, Jeongho Park, and Songhwai Oh. Topological semantic graph memory for image-goal navigation. In *Conference on Robot Learning*, pages 393–402. PMLR, 2023. 1

[21] Andrey Kurenkov, Michael Lingelbach, Tanmay Agarwal, Emily Jin, Chengshu Li, Ruohan Zhang, Li Fei-Fei, Jiajun Wu, Silvio Savarese, and Roberto Martın-Martın. Modeling dynamic environments with scene graph memory. In *International Conference on Machine Learning*, pages 17976–17993. PMLR, 2023. 3

[22] Dong Li, Qichao Zhang, and Dongbin Zhao. Graph attention memory for visual navigation. In *2022 4th International Conference on Data-driven Optimization of Complex Systems (DOCS)*, pages 1–7. IEEE, 2022. 1

[23] Jialu Li, Hao Tan, and Mohit Bansal. Improving cross-modal alignment in vision language navigation via syntactic information. *arXiv preprint arXiv:2104.09580*, 2021. 1

[24] Liunian Harold Li, Pengchuan Zhang, Haotian Zhang, Jianwei Yang, Chunyuan Li, Yiwu Zhong, Lijuan Wang, Lu Yuan, Lei Zhang, Jenq-Neng Hwang, Kai-Wei Chang, and Jianfeng Gao. Grounded Language-Image Pre-training, 2022. 2, 4

[25] Weiyuan Li, Ruoxin Hong, Jiwei Shen, Liang Yuan, and Yue Lu. Transformer memory for interactive visual navigation in cluttered environments. *IEEE Robotics and Automation Letters*, 8(3):1731–1738, 2023. 3

[26] Jinzhou Lin, Han Gao, Xuxiang Feng, Rongtao Xu, Changwei Wang, Man Zhang, Li Guo, and Shibiao Xu. Advances in embodied navigation using large language models: A survey. *arXiv preprint arXiv:2311.00530*, 2023. 1

[27] Haotian Liu, Chunyuan Li, Yuheng Li, and Yong Jae Lee. Improved baselines with visual instruction tuning. In *Proceedings of the IEEE/CVF Conference on Computer Vision and Pattern Recognition*, pages 26296–26306, 2024. 2

[28] Haotian Liu, Chunyuan Li, Qingyang Wu, and Yong Jae Lee. Visual instruction tuning. *Advances in neural information processing systems*, 36, 2024. 2

[29] Christoforos I Mavrogiannis and Ross A Knepper. Decentralized multi-agent navigation planning with braids. In *Algorithmic Foundations of Robotics XII: Proceedings of the Twelfth Workshop on the Algorithmic Foundations of Robotics*, pages 880–895. Springer, 2020. 2

[30] Matthias Minderer, Alexey Gritsenko, Austin Stone, Maxim Neumann, Dirk Weissenborn, Alexey Dosovitskiy, Aravindh Mahendran, Anurag Arnab, Mostafa Dehghani, Zhuoran Shen, Xiao Wang, Xiaohua Zhai, Thomas Kipf, and Neil Houlsby. Simple open-vocabulary object detection with vision transformers, 2022. 2, 4

[31] M.G. Mohanan and Ambuja Salgoankar. A survey of robotic motion planning in dynamic environments. *Robotics and Autonomous Systems*, 100:171–185, 2018. 2

[32] Timothy Morris, Feras Dayoub, Peter Corke, Gordon Wyeth, and Ben Upcroft. Multiple map hypotheses for planning and navigating in non-stationary environments. In *2014 IEEE international conference on robotics and automation (ICRA)*, pages 2765–2770. IEEE, 2014. 3

[33] Soroush Nasiriany, Fei Xia, Wenhao Yu, Ted Xiao, Jacky Liang, Ishita Dasgupta, Annie Xie, Danny Driess, Ayzaan Wahid, Zhuo Xu, et al. Pivot: Iterative visual prompting elicits actionable knowledge for vlms. *arXiv preprint arXiv:2402.07872*, 2024. 2

[34] Maithili Patel and Sonia Chernova. Proactive robot assistance via spatio-temporal object modeling. *arXiv preprint arXiv:2211.15501*, 2022. 1, 5

[35] Xavier Puig, Eric Undersander, Andrew Szot, Mikael Dallaire Cote, Tsung-Yen Yang, Ruslan Partsey, Ruta Desai, Alexander William Clegg, Michal Hlavac, So Yeon Min, et al. Habitat 3.0: A co-habitat for humans, avatars and robots. *arXiv preprint arXiv:2310.13724*, 2023. 2

[36] Yuankai Qi, Qi Wu, Peter Anderson, Xin Wang, William Yang Wang, Chunhua Shen, and Anton van den Hengel. REVERIE: Remote Embodied Visual Referring Expression in Real Indoor Environments, 2020. 1

[37] Santhosh K Ramakrishnan, Aaron Gokaslan, Erik Wijmans, Oleksandr Maksymets, Alex Clegg, John Turner, Eric Undersander, Wojciech Galuba, Andrew Westbury, Angel X Chang, et al. Habitat-matterport 3d dataset (hm3d): 1000 large-scale 3d environments for embodied ai. *arXiv preprint arXiv:2109.08238*, 2021. 2

[38] Ram Ramrakhya, Eric Undersander, Dhruv Batra, and Abhishek Das. Habitat-web: Learning embodied object-search strategies from human demonstrations at scale. In *Proceedings of the IEEE/CVF Conference on Computer Vision and Pattern Recognition*, pages 5173–5183, 2022. 1

[39] Evan F Risko and Sam J Gilbert. Cognitive offloading. *Trends in cognitive sciences*, 20(9):676–688, 2016. 3

[40] Sohan Rudra, Saksham Goel, Anirban Santara, Claudio Gentile, Laurent Perron, Fei Xia, Vikas Sindhwani, Carolina Parada, and Gaurav Aggarwal. A contextual bandit approach for learning to plan in environments with probabilistic goal configurations. In *2023 IEEE International Conference on Robotics and Automation (ICRA)*, pages 5645–5652. IEEE, 2023. 3

[41] Adarsh Jagan Sathyamoorthy, Jing Liang, Utsav Patel, Tianrui Guan, Rohan Chandra, and Dinesh Manocha. Densecavoid: Real-time navigation in dense crowds using anticipatory behaviors. In *2020 IEEE International Conference on Robotics and Automation (ICRA)*, pages 11345–11352. IEEE, 2020. 2

[42] Adarsh Jagan Sathyamoorthy, Kasun Weerakoon, Mohamed Elnoor, Anuj Zore, Brian Ichter, Fei Xia, Jie Tan, Wenhao Yu, and Dinesh Manocha. Convoi: Context-aware navigation using vision language models in outdoor and indoor environments. *arXiv preprint arXiv:2403.15637*, 2024. 2

[43] John Schulman, Filip Wolski, Prafulla Dhariwal, Alec Radford, and Oleg Klimov. Proximal policy optimization algorithms. *arXiv preprint arXiv:1707.06347*, 2017. 6

[44] Dhruv Shah, Benjamin Eysenbach, Gregory Kahn, Nicholas Rhinehart, and Sergey Levine. Ving: Learning open-world navigation with visual goals. In *2021 IEEE International Conference on Robotics and Automation (ICRA)*, pages 13215–13222. IEEE, 2021. 2

[45] Dhruv Shah, Blazej Osinski, Brian Ichter, and Sergey Levine. LM-Nav: Robotic Navigation with Large Pre-Trained Models of Language, Vision, and Action, 2022. 1

[46] Kyle S Smith and Ann M Graybiel. Habit formation. *Dialogues in clinical neuroscience*, 18(1):33–43, 2016. 3

[47] Richard S Sutton, Andrew G Barto, et al. *Reinforcement learning: An introduction*. MIT press Cambridge, 1998. 1

[48] Victor Vladareanu, Gabriela Tont, Luige Vladareanu, and Florentin Smarandache. The navigation of mobile robots in non-stationary and non-structured environments. *International Journal of Advanced Mechatronic Systems*, 5(4):232–242, 2013. 3

[49] Chenxu Wang, Xinghang Li, Dunzheng Wang, Huaping Liu, et al. Dynamic scene generation for embodied navigation benchmark. In *RSS 2024 Workshop: Data Generation for Robotics*, 2024. 3

[50] Saim Wani, Shivansh Patel, Unnat Jain, Angel Chang, and Manolis Savva. Multion benchmarking semantic map memory using multi-object navigation. *Advances in Neural Information Processing Systems*, 33:9700–9712, 2020. 1, 5, 7

[51] Erik Wijmans, Abhishek Kadian, Ari Morcos, Stefan Lee, Irfan Essa, Devi Parikh, Manolis Savva, and Dhruv Batra. Dd-ppo: Learning near-perfect pointgoal navigators from 2.5 billion frames. *arXiv preprint arXiv:1911.00357*, 2019. 6

[52] Erik Wijmans, Abhishek Kadian, Ari Morcos, Stefan Lee, Irfan Essa, Devi Parikh, Manolis Savva, and Dhruv Batra. Dd-ppo: Learning near-perfect pointgoal navigators from 2.5 billion frames, 2020. 1

[53] Rey Reza Wiyatno, Anqi Xu, and Liam Paull. Lifelong topological visual navigation. *IEEE Robotics and Automation Letters*, 7(4):9271–9278, 2022. 1, 5

[54] Karmesh Yadav, Arjun Majumdar, Ram Ramrakhya, Naoki Yokoyama, Alexei Baevski, Zsolt Kira, Oleksandr Maksymets, and Dhruv Batra. Ovrl-v2: A simple state-of-art baseline for imagenav and objectnav. *arXiv preprint arXiv:2303.07798*, 2023. 1, 6

[55] Hwiyeon Yoo, Yunho Choi, Jeongho Park, and Songhwai Oh. Commonsense-aware object value graph for object goal navigation. *IEEE Robotics and Automation Letters*, 2024. 1

[56] Xu Zhao, Wenchao Ding, Yongqi An, Yinglong Du, Tao Yu, Min Li, Ming Tang, and Jinqiao Wang. Fast segment anything. *arXiv preprint arXiv:2306.12156*, 2023. 5, 2

[57] Duo Zheng, Shijia Huang, Lin Zhao, Yiwu Zhong, and Liwei Wang. Towards learning a generalist model for embodied navigation. In *Proceedings of the IEEE/CVF Conference on Computer Vision and Pattern Recognition*, pages 13624–13634, 2024. 1

[58] Yan Zheng, Zhaopeng Meng, Jianye Hao, Zongzhang Zhang, Tianpei Yang, and Changjie Fan. A deep bayesian policy reuse approach against non-stationary agents. *Advances in neural information processing systems*, 31, 2018. 3

[59] Ye Zhou and Hann Woei Ho. Online robot guidance and navigation in non-stationary environment with hybrid hierarchical reinforcement learning. *Engineering Applications of Artificial Intelligence*, 114:105152, 2022. 3

[60] Hao Zhu, Raghav Kapoor, So Yeon Min, Winson Han, Jiatai Li, Kaiwen Geng, Graham Neubig, Yonatan Bisk, Aniruddha Kembhavi, and Luca Weihs. Excalibur: Encouraging and evaluating embodied exploration. In *Proceedings of the IEEE/CVF Conference on Computer Vision and Pattern Recognition*, pages 14931–14942, 2023. 6

Right Place, Right Time!
Dynamizing Topological Graphs for Embodied Navigation

Supplementary Material

Supplementary Material

8. Dataset Details

While the agents introduced in Section 2 tackle the *temporal* dynamism, i.e., identifying *where* and *when* the target object is likely to lie at a particular location, visual grounding is a separate task tackling *spatial* dynamism. An ideal agent performs both these tasks *simultaneously*, verifying at each timestep if a portable target exists by running a grounding model. As navigation decisions are not directly impacted by the performance of a grounding model, we study temporal and spatial dynamism independently.

The dataset contains temporal and spatial modifications on the Matterport3D scans. Further, we provide code and useful tools for implementing these modifications.

Scan ID	# of Nodes	# of Edges	# of Rooms
QUCTc6BB5sX	145	248	28
8194nk5LbLH	20	32	6
TbHJrupSAjP	114	221	28
2azQ1b91cZZ	215	531	30
oLBMNvg9in8	111	185	31
zsNo4HB9uLZ	53	84	17
EU6Fwq7SyZv	78	166	19
X7HyMhZNoso	84	143	25
x8F5xyUWy9e	43	86	10
Z6MFQCViBuw	58	91	18

Table 4. Summary statistics of scans used for Table 3, including each scan's ID, number of nodes, edges, and rooms. If a scan has multiple rooms of the same type (e.g. two bathrooms), each instance is counted separately from the total.

For the spatial placement, we provide a dataset of $10,500$ modified images taken across 10 randomly chosen Matterport3D scans, with 21 portable objects randomly oriented and positioned 5 times within each image. Table 4 summarizes the different Matterport3D scans chosen. To emulate realism such that the portable objects are not floating in the sky or on the ceiling, they are placed on a large segmented area below the center of the image. We also provide the bounding boxes pertaining to the portable object in each image.

8.1. Temporal: Implementing Object Placement Strategies

In this section, we give more details on how we implemented the dynamic Matterport3D environment.

Matterport3D Modifications:

Each Matterport3D (MP3D) scan represents a household environment consisting of a set of panoramic view points. Along with the viewpoints (or nodes), we are also given the exact 3D position as well as the relative distance between them. For modifying the MP3D environment, we first construct topological graphs of each scan, with nodes containing the position and the panoramic image, and edges containing relative distance between them. We consider 10 different scans chosen from the REVERIE [36] and R2R [2] unseen validation splits for inference. We choose scans according to these datasets as they contain a variety of rooms for us to populate (Refer Table 1 in the main paper).

The nodes of the topological graphs are then updated at each timestep with the portable objects according to the object placement scenario that has been chosen.

Strategy Overview:

We compute trajectories of the portable objects in an offline manner. For a fixed random seed s and for each portable object $o_p \in O_p$, we create a sequence of nodes from the graph. In the random transit scenario, we choose any node in the graph. In the routine and semi-routine scenarios, we only choose nodes from plausible rooms. If the node chosen is not the same as the current node, we find the shortest path between the current node and the target node and add the nodes in the path to the sequence representing the trajectory. Once o_p gets to the target node, it stays there for either 2 or 3 timesteps, determined by a random number generator. For each timestep o_p stays at the node, we add the node to the trajectory sequence. After the staying period is over we select a new node and repeat the process until we hit T timesteps.

We take the resulting trajectories and restructure the data to model an evolving graph over a period of T timesteps. The resulting structure is a nested dictionary representing the changing graph. The keys of the outer dictionary are the timesteps $[1, ..., T]$. The inner dictionary for each timestep t has the node string ids as the keys and the values are the list of portable objects at that node at T. At each timestep $t \in [1, ..., T]$ when the agent reaches a node, we simply use t and the node id to retrieve the list of portable objects the agent is currently observing.

8.2. Spatial: Implementing Visual Grounding

In this section, we talk about our strategy for spatial placement of multiple portable target objects on MP3D scenes. After placing portable objects at various locations, we perform visual grounding using three Open-World Object Detection models for inference. We also show further ablations using VLMs.

Generating Spatial Data:

We randomly choose 100 skybox images taken across the 10 MP3D scans mentioned in the previous subsection. While selecting these images are not of the ceiling or the floor, and have objects pertaining everyday scenes. We then pick stock images of all the 21 portable objects present in Table 1 of the main manuscript. These images are shown in Figure 10.

For each of the skybox images, we first run FastSAM [56] and segment out the largest regions below the center of the image. We then randomly orient the portable object and place it at a random position on one of these segments. Choosing segments below the center of the image is necessary to ensure that the portable objects being placed follow commonsense, and do not hang in the ceiling. This is done 5 times for each of the 21 objects on 100 images, to get 10500 images in total. While placing the images, we also store the boundaries of the overlay as the ground truth bounding box for computing Intersection over Union (IOU) scores.

Examples of this generated data is shown in Figure 8. Note that the same image can have multiple target segmentations (*bed* and *cushion* for example), with different objects placed on them at different orientations.

Open-World Visual Object Grounding

We perform Visual Grounding on the spatial placement dataset using various Open-Vocabulary Object Detection Models. For each model, we assess the **Detection Coverage**, which is the percentage of images where the portable object was found, the **Detection Accuracy**, the accuracy of the predicted detections, and finally **Mean IOU**, which gives us the overlap between the ground truth bounding box of the placed target and the predicted box. The results for this are shown in Table 5.

We make some interesting observations. OWL-ViT [30] outperforms GLIP [24] and YOLO-World [12] when it comes to Detection Coverage, which means that it consistently detects an object, irrespective of whether it is right or wrong on the image. This is evident since it takes a target object label is given as a prompt to OWL-ViT, so it detects something in the image, even if the confidence is low. Figure 5 shows some examples of this.

GLIP, while having lower detection coverage, has a perfect detection accuracy, meaning that when GLIP does detect something, it usually is correct. The high MIOU score associated with GLIP also corroborates with this fact. Figure 6 shows some example results of this.

We infer the YOLO-World model with custom vocabulary consisting of all the portable object names. Despite this, YOLO still performs the worst among the three, with poor detection accuracy and coverage. Figure 7 showcases one of these results. Notice that in the first image screwdriver is grounded at the right location, but the label is "Cow". In the second image, both the predicted target (fire hydrant) and the grounding is wrong.

We note that the poor detection as measured by MIOU could be a result of unnatural scenes that are different from those which these models might have been trained on. Beyond this, grounding small, portable targets that could be present on various surfaces in a household environment still remains a challenge. We will be releasing this dataset to foster research in this area.

8.3. Spatial Reasoning with Vision Language Models (VLMs)

We perform visual grounding using 4 popular Vision Language Models (VLMs): InstructBLIP [28], LLaVA 1.5 [27] and GPT-4o [1]. For InstructBLIP, we experiment with two different language backends: Flan-T5, which has been fine-tuned on various language tasks including question answering, and Vicuna-13B, which has been trained specifically on conversational data.

Figure 11 illustrates the images we pass to these models to validate their spatial reasoning capability. Given an image containing a small portable target for grounding, we first paste a number grid from $[1-9]$ onto the image. Prior research by Sathyamoorthy et. al [42] and Nasiriany et. al [33] has utilized this technique to guide robots in indoor as well as outdoor scenarios.

In our case, we evaluate a subset of 1000 images in our dataset containing various objects by asking each image the query - " Where is the <*objects*> in this image? Reply with the corresponding grid number from [1-9].", and then evaluate the response we get with the ground truth. Since we create the dataset by pasting target objects onto them, this is readily available to us. Table 6 presents the accuracies for this task the various VLMs.

9. Experimental Details

9.1. LGX Inference

We utilize the official implementation of LGX [1] and incorporate it into our modified MP3D environment. Briefly, at each timestep, LGX scans the node for objects, and asks an LLM for directions to reach a target. In our case, we seek to maximize finding portable targets. As such, we prompt GPT-4 with the following base prompts -

> **System Prompt** - "I am a smart robot trying to find as many portable objects as I can at home."
> **User Prompt** - "Which object from <*OBJECT_LIST*> should I go towards to find a new portable object? Reply in ONE word."

The <OBJECT_LIST> here contains a set of objects that have been detected using YOLO-v8, as proposed in

[1]https://github.com/vdorbala/LGX

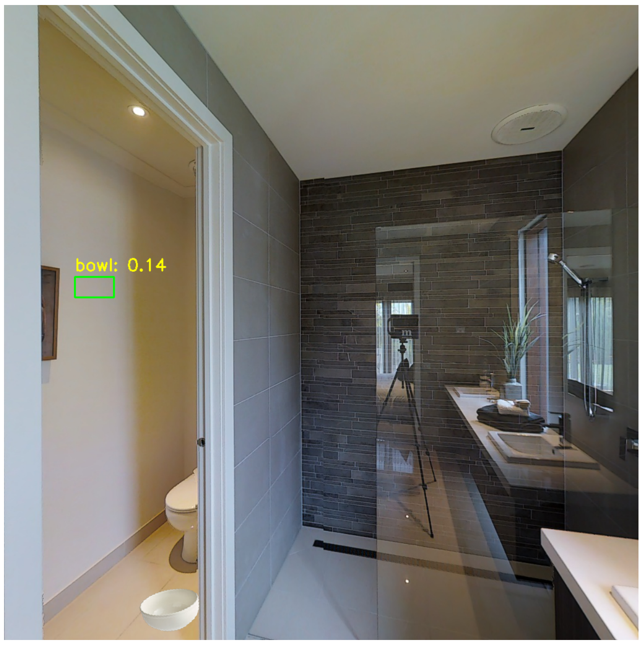

(**a**) Portable Target: Bowl

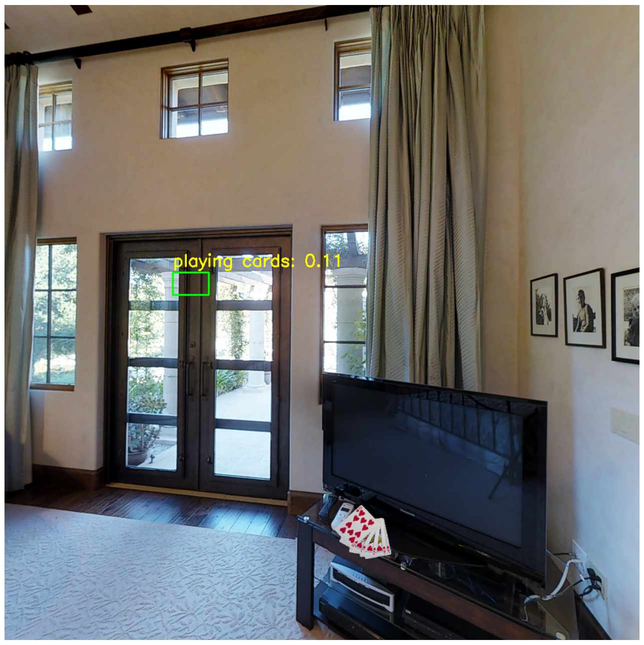

(**b**) Portable Target: Playing Cards

Figure 5. OWL-ViT Detection Failures: Note the poor detection accuracy of OWL-ViT. On both images, it completely misses the object when prompted with a text containing the target label. We attribute these failures to unnatural images being generated by pasting target objects onto the scene.

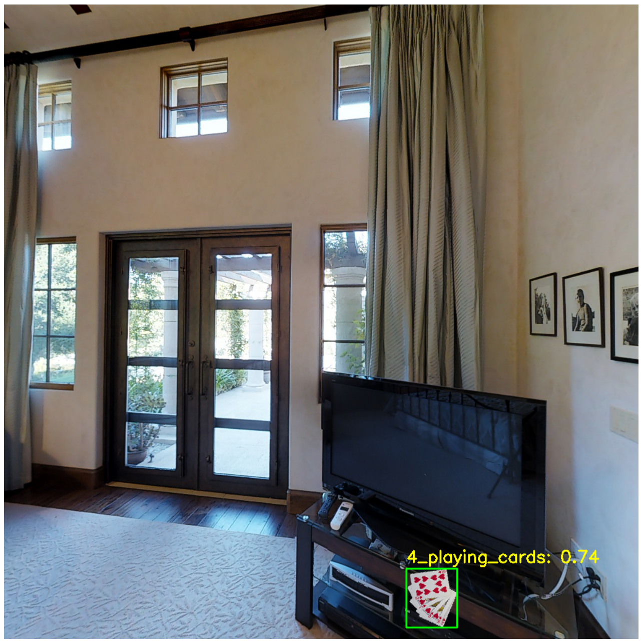

(**a**) Portable Target: Playing Cards

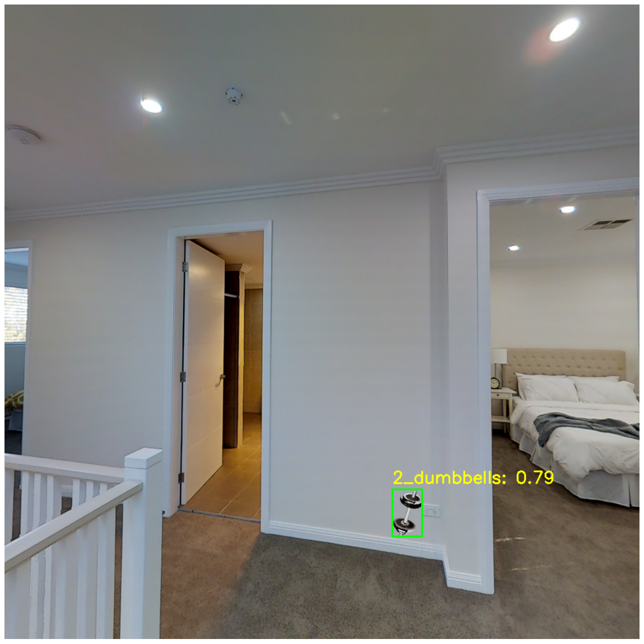

(**b**) Portable Target: Dumbbells

Figure 6. GLIP Detection Accuracy: Note the superior detection accuracy, despite the low coverage on GLIP. On the image on the laft and right, playing cards and dumbbells are detected correctly with a high accuracy.

LGX. Additionally, we if a portable object is present at a certain node at a given timestep, we add it to this list.

The LLM then predicts a target object from the list, which is mapped to an adjacent node using our customized MP3D functions.

For the **memory-enhanced** LGX case, we modify the System Prompt, with memory. We additionally ask -

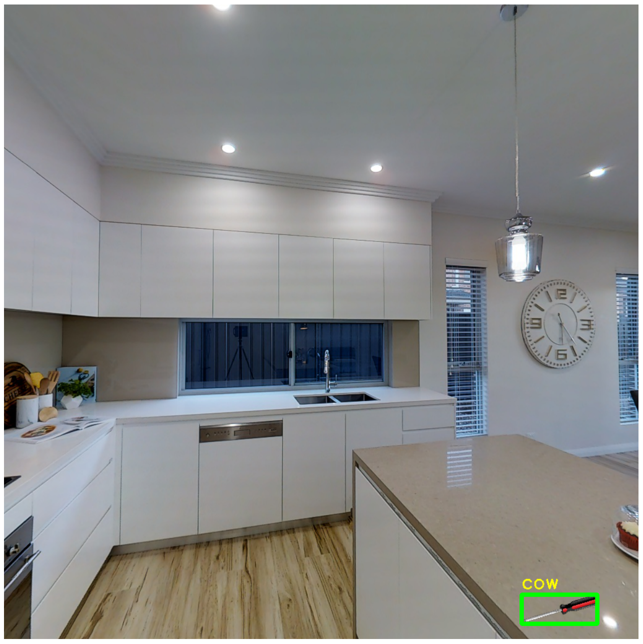

(a) Portable Target: Screwdriver

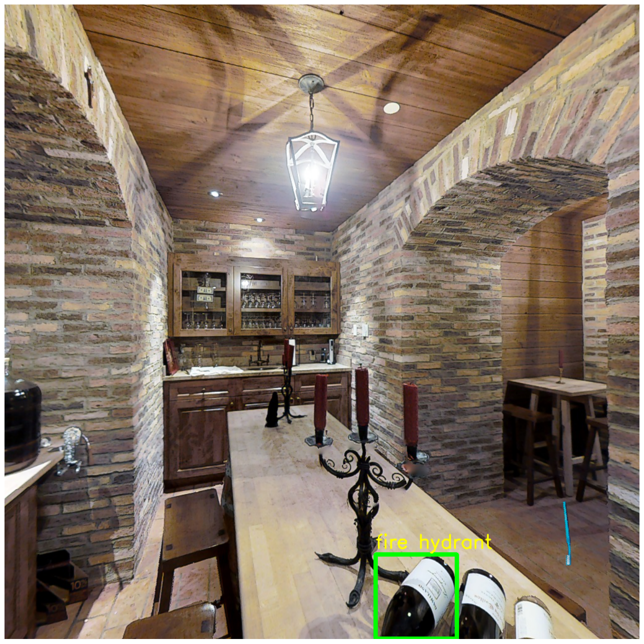

(b) Portable Target: Toothbrush

Figure 7. YOLO Detection Failures: Note the poor detection accuracy of YOLO. On the image on the left, the screwdriver is grounded correctly, but the object name predicted is "Cow". On the image on the right, YOLO completely misses the target object toothbrush, and instead grounds and labels something else.

Approach	Detection Coverage	Detection Accuracy	MIOU
OWL-ViT[30]	**100%**	3.04%	0.352
GLIP [24]	7.11%	**100%**	**0.489**
YOLO-World [12]	32.94%	0.2%	0.130

Table 5. Comparison of Open-World Object Detaction Approaches

Model	**Accuracy (%)**
InstructBLIP + Vicuna-7B	15.38
InstructBLIP + Flan-T5-XL	4.32
LLaVA v1.5 + Vicuna 13B	58.62
GPT 4o-mini	75.89
GPT 4o	**98.32**

Table 6. VQA Model Accuracies: Note the superior performance of GPT 4o on our number grid based spatial reasoning task. The remaining VLMs show inferior performance, with a Vicuna backend performing better than the Flan one; this can be attributed to Vicuna being predominantly trained on conversational data that might contain such queries.

System Prompt:
"I have seen the following objects and taken the following actions so far -
1. <OBJECT_LIST>: ACTION
2. <OBJECT_LIST>: ACTION
. . ."

User Prompt:
"Which object from <*OBJECT_LIST*> should I go towards to find a new portable object? Reply in ONE word."

10. Code and Dataset

We provide an anonymous link to our Code: `https://anonymous.4open.science/r/otg-1AC0`. The dataset will be present as a downloadable link in the code repository.

Furthermore, please see the attached video in the zip file for more information and demonstrations.

(a) Dice on Bed

(b) Mug on Cushion

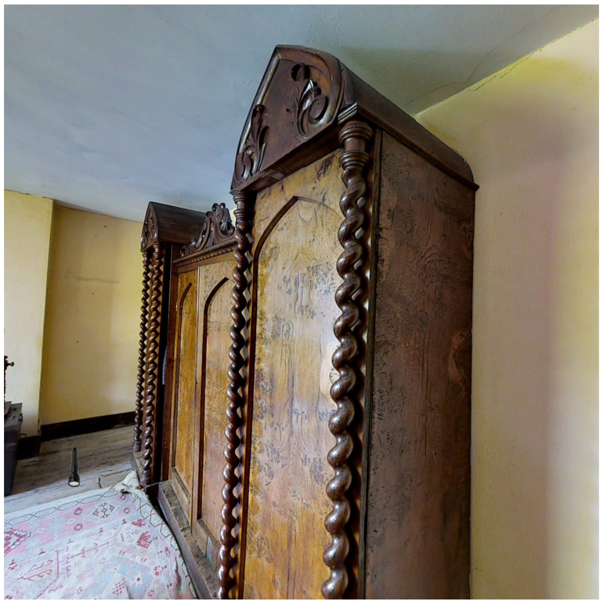
(c) Flashlight on Floor

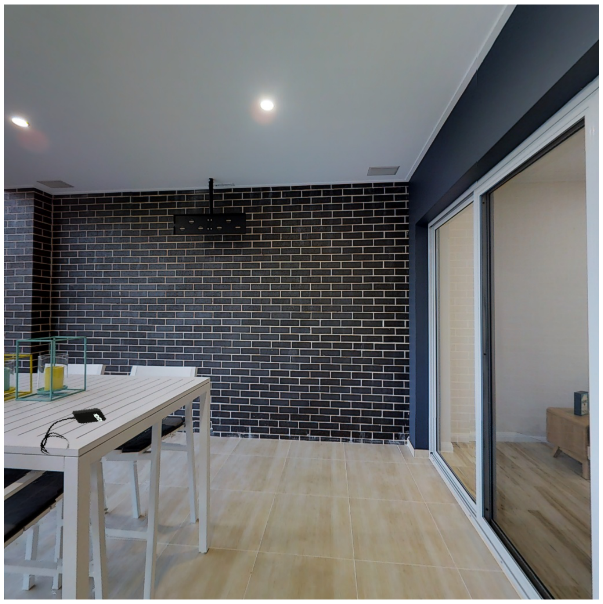
(d) Charger on Table

Figure 8. Various Spatial Placement in our Dataset: Figures (a) and (b) look at different arrangements of objects in the same room. Figure (c) shows a flashlight on the floor, and figure (d) shows a charger on the table. We cover various orientations and rotations of portable objects being placed on various objects in different MP3D scans.

(a) bowl

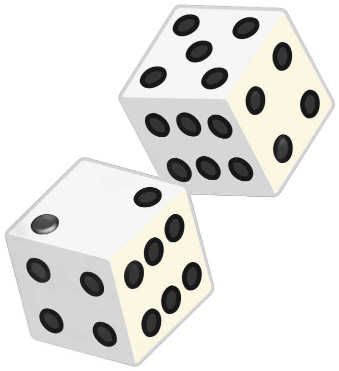
(b) dice

(c) dumbbell

(d) flashlight

(e) glasses

(f) hat

(g) salt and pepper shakers

(h) screwdriver

(i) toothbrush

(j) remote

(k) playing cards

(l) phone

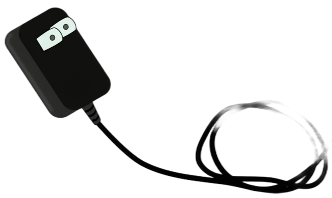
(m) phone charger

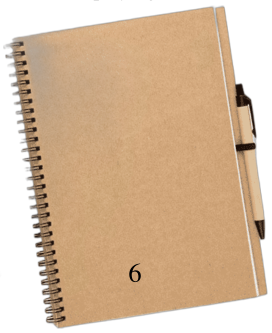
(n) notebook

(o) mug

(a) laptop

(b) jumprope

(c) headphones

(d) wallet

(e) water bottle

(f) wristwatch

Figure 10. Portable Objects: A list of all the 21 portable objects we consider for our task.

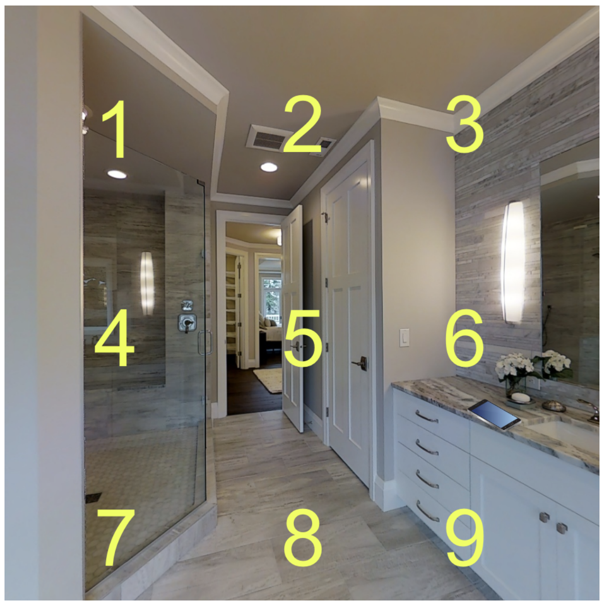

(a) Phone in bathroom

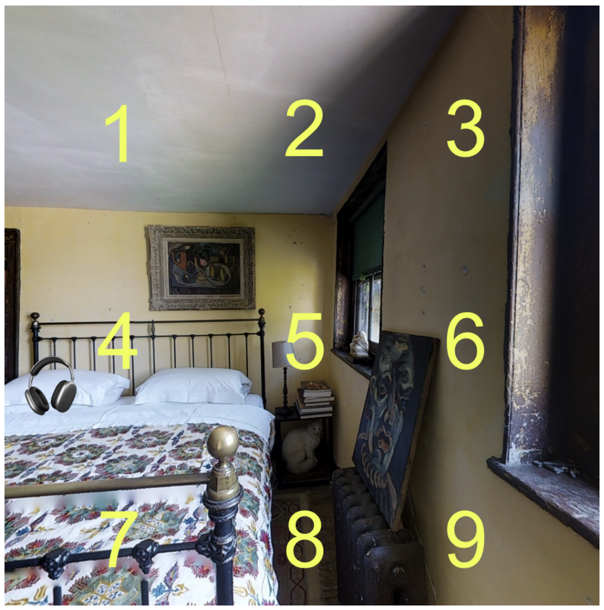

(b) Headphones on bed

Figure 11. We evaluate the spatial reasoning capabilities of VLMs in grounding small portable targets in houses. The question we ask is "What is the closest number to the <INSERT OBJECT> in this image?" and it answers with a number.